different edges on top of the monotonously decaying background is a signature of the elemental composition, the intensity of the signals being roughly proportional to the relative concentration in the associated element. Core-level EELS spectroscopy therefore investigates transitions from one well defined atomic orbital to a vacant state above the Fermi level: it is a probe of the energy distribution of vacant states in a solid, see Fig. 4.3.4.5. As the excited electron is promoted on a given atomic site, the information involved has two specific characters: it provides the local atomic point of view and it reflects the existence of the hole created, which can be more or less screened by the surrounding population of electrons in the solid. The properties of this family of excitations are the subject of Subsection 4.3.4.4.

The non-characteristic background is due to the superposition of several contributions: the high-energy tail of valence-electron scattering, the tails of core losses with lower binding energy, *Bremsstrahlung* energy losses, plural scattering, *etc*. It is therefore rather difficult to model its behaviour, although some efforts have been made along this direction using Monte Carlo simulation of multiple scattering (Jouffrey, Sevely, Zanchi & Kihn, 1985).

When one monochromatizes the natural energy width of the primary beam to much smaller values (about a few meV) than its natural width, one has access to the infrared part of the electromagnetic spectrum. An example is provided in Fig. 4.3.4.6 for a specimen of germanium in the energy-loss range 0 up to 500 meV. In this case, one can investigate phonon modes, or the bonding states of impurities on surfaces. This field has been much less extensively studied than the higher-energy-loss range [for references see Ibach & Mills (1982)].

Generally, EELS techniques can be applied to a large variety of specimens. However, for the following review to remain of limited size, it is restricted to electron energy-loss spectroscopy on solids and surfaces in transmission and reflection. It omits some important aspects such as electron energy-loss spectroscopy in gases with its associated information on atomic and molecular states. In this domain, a bibliography of inner-shell excitation studies of atoms and molecules by electrons, photons or theory is available from Hitchcock (1982).

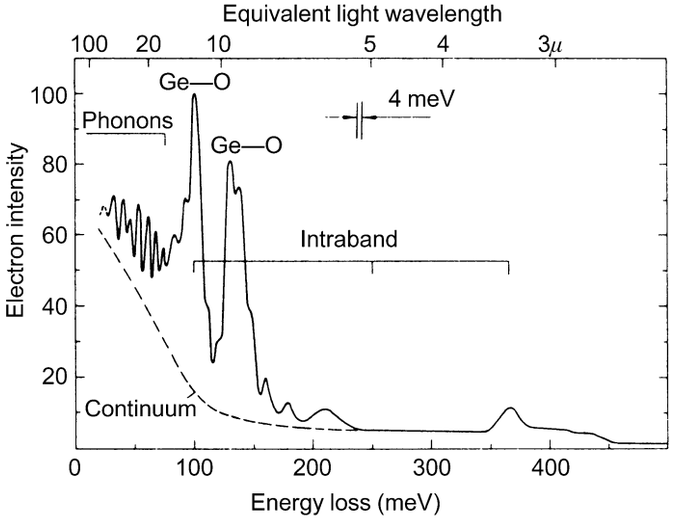

Fig. 4.3.4.6. Energy-loss spectrum, in the meV region, of an evaporated germanium film (thickness $\simeq 25$ nm). Primary electron energy 25 keV. Scattering angle $< 10^{-4}$. One detects the contributions of the phonon excitation, of the Ge—O bonding, and of intraband transitions [courtesy of Schröder & Geiger (1972)].

Table 4.3.4.1. *Different possibilities for using EELS information as a function of the different accessible parameters* (**r**, θ, ΔE)

	Integration parameter	Selection parameter	Results	Working mode of the spectrometer
1	**θ**	**r**	Spectrum $I_{\mathbf{r}}$ (ΔE)	Analyser
2	**r**	**θ**	Spectrum $I_{\boldsymbol{\theta}}$ (ΔE)	Analyser
3	**θ**	ΔE	Energy-filtered image $I_{\Delta E}(\mathbf{r})$	Filter
4	**r**	ΔE	Energy-filtered diffraction pattern $I_{\Delta E}(\boldsymbol{\theta})$	Filter

4.3.4.2. *Instrumentation*

4.3.4.2.1. *General instrumental considerations*

In a dedicated instrument for electron inelastic scattering studies, one aims at the best momentum and energy resolution with a well collimated and monochromatized primary beam. This is achieved at the cost of poor spatial localization of the incident electrons and one assumes the specimens to be homogeneous over the whole irradiated volume. In a sophisticated instrument such as that built by Fink & Kisker (1980), the energy resolution can be varied from 0.08 to 0.7 eV, and the momentum transfer resolution between 0.03 and 0.2 Å^{-1}, but typical values for the electron-beam diameter are about 0.2 to 1 mm. Nowadays, many energy-analysing devices are coupled with an electron microscope: consequently, an inelastic scattering study involves recording for a primary intensity I_0, the current $I(\mathbf{r}, \boldsymbol{\theta}, \Delta E)$ scattered or transmitted at the position **r** on the specimen, in the direction **θ** with respect to the primary beam, and with an energy loss ΔE. Spatial resolution is achieved either with a focused probe or by a selected area method, angular acceptance is defined by an aperture, and energy width is controlled by a detector function after the spectrometer. It is not possible from signal-to-noise considerations to reduce simultaneously all instrumental widths to very small values. One of the parameters (**r**, **θ** or ΔE) is chosen for signal integration, another for selection, and the last is the variable. Table 4.3.4.1. classifies these different possibilities for inelastic scattering studies.

Because of the great variety of possible EELS experiments, it is impossible to build an optimum spectrometer for all applications. For instance, the design of a spectrometer for low-energy incident electrons and surface studies is different from that for high-energy incident electrons and transmission work. In the latter category, instruments built for dedicated EELS studies (Killat, 1974; Gibbons, Ritsko & Schnatterly, 1975; Fink & Kisker, 1980; *etc*.) are different from those inserted within an electron-microscope environment, in which case it is possible to investigate the excitation spectrum from a specimen area well characterized in image and diffraction [see the reviews by Colliex (1984) and Egerton (1986)].

The literature on dispersive electron–optical systems (equivalent to optical prisms) is very large. For example, the theory of uniform field magnets, which constitute an important family of analysing devices, has been extensively developed for the components in high-energy particle accelerators (Enge, 1967; Livingood, 1969). As for EELS spectrometers, they can be classified as:

(*a*) *Monochromators*, which filter the incident beam to obtain the smallest primary energy width. The natural width for a heated W filament is about 1 eV, possibly rising to about a few eV as a consequence of stochastic interactions [Boersch (1954) effect, analysed for instance by Rose & Spehr (1980)]. For a low-temperature field-emission source, this energy spread is only ~0.3 eV. This constitutes a clear gain but remains insufficient for meV studies. In this case, one has to introduce a filter lens such as the three-electrode design developed by Hartl (1966) or a cylindrical electrostatic deflector before the accelerator [Kuyatt & Simpson (1967) or Gibbons *et al.* (1975)]. In both cases, an energy resolution of 50 meV has been achieved for electron beams of 50–300 keV at the specimen.

(*b*) *Analysers*, which measure the energy distribution of the beam scattered from the specimen. They can be used either strictly as analysers displaying the energy loss from a given specimen volume, or as filters (or selecting devices) that provide 2D images or diffraction patterns with a given energy loss.

4.3.4.2.2. *Spectrometers*

Fig. 4.3.4.7 defines the basic parameters of a 'general' energy-loss spectrometer: a region of electrostatic **E** and/or magnetic **B** fields transforms a distribution of electrons $I_0(x_0, y_0, t_0, u_0, \rho)$ in the object plane of coordinate z_0 along the principal trajectory, into a distribution of electrons $I_1(x_1, y_1, t_1, u_1, \rho)$ in the object plane of coordinate z_1, coincident with the detector plane (or optically conjugate to it). The transverse coordinates are labelled as (x, y), the angular ones as (t, u), and $\rho = \Delta p/p = \Delta E/2E$ is the relative change in absolute momentum value associated with the energy loss.

Common properties of such systems are:

(*a*) first-order imaging properties or stigmatism, *i.e.* all electrons leaving (x_0, y_0) are focused at the same (x_1, y_1) point, independently of their inclination on the optical axis;

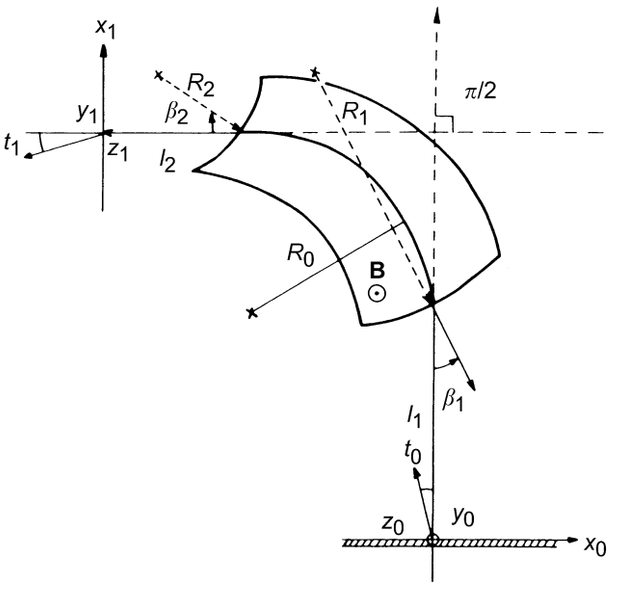

Fig. 4.3.4.7. Schematic drawing of a uniform magnetic sector spectrometer with induction **B** normal to the plane of the figure. Definition of the coordinates used in the text (the object plane at coordinate z_0 along the mean trajectory coincides with the specimen, and the image plane at z_1 coincides with the dispersion plane and the detector level).

(*b*) strong chromatic aberration in order to realize an efficient discrimination between electrons of different ρ.

The spectrometer performance can be evaluated with the following parameters:

D = *dispersion* = beam displacement in the spectrometer image plane for a given momentum change ρ; it is generally expressed in cm/eV. The higher the dispersion, the easier it is to resolve small energy losses. For a straight-edge 90° magnetic sector, $D \propto 2R/E_0$, where R is the curvature radius of the mean trajectory and E_0 is the primary energy.

$\delta E_{\min}$ = *energy resolution*. This corresponds to the minimum-energy variation that can be resolved by the instrument. It takes into account the width of the image $\Delta x_{\text{image}} = Mr$, where M is the spectrometer magnification and r the radius of the spectrometer source, as well as the second- and higher-order angular aberrations. These are responsible for the imperfect focusing of the electrons that enter the spectrometer within a cone of angular acceptance β_0 and contribute through a term $\Delta x_{\text{aber}} = C\beta_0^2$. Moreover, one must convolute these terms with the natural width δE_0 of the primary beam, including AC fields, and with the detection slit width Δx_{slit}. Combining all these effects, as shown schematically in Fig. 4.3.4.8, one obtains approximately:

$$\Delta x_{\text{tot}} = [(\Delta x_{\text{slit}})^2 + (\Delta x_{\text{image}})^2 + (\Delta x_{\text{aber}})^2 + D\delta E_0^2]^{1/2} \quad (4.3.4.7)$$

and the corresponding energy resolution is defined as $\delta E_{\min} = (\Delta x_{\text{tot}})_{\min}/D$. In many situations, the dominant factor is the second-order aberration term $C\beta_0^2$ so that the figure of merit F, defined as $F = \pi\beta_0 E_0/\delta E_{\min}$, is of the order of unity for an uncorrected magnetic spectrometer.

From this simplified discussion, one deduces that there is generally competition between large angular acceptance for the inelastic signal, which is very important for obtaining a high signal-to-noise ratio (SNR) for core-level excitations, and good energy resolution. Two solutions have been used to remedy this limitation. The first is to improve spectrometer design, for example by correcting second-order aberrations in a homogeneous magnetic prism (Crewe, 1977*a*; Parker, Utlaut & Isaacson, 1978; Egerton, 1980*b*; Krivanek & Swann, 1981; *etc*). This can enhance the figure of merit by at least a factor of 100. The second possibility is to transform the distribution of electrons to be analysed at the exit surface of the specimen into a more convenient distribution at the spectrometer entrance. This can be done by introducing versatile transfer optics (see Crewe, 1977*b*; Egerton, 1980*a*; Johnson, 1980; Craven & Buggy, 1981; *etc*.). As a final remark on the energy resolution of a spectrometer, it is meaningless to define it without reference to the size and the angular aperture of the analysed beam.

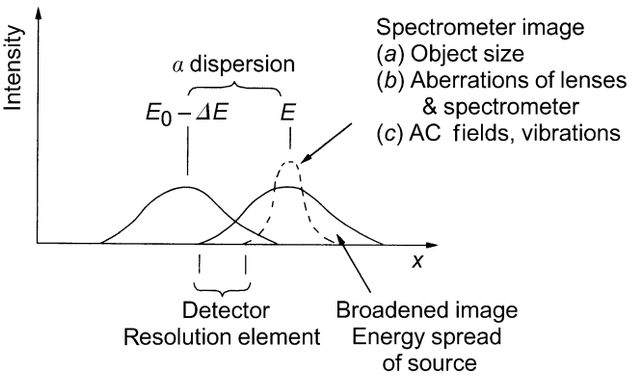

Fig. 4.3.4.8. Different factors contributing to the energy resolution in the dispersion plane [courtesy of Johnson (1979)].

references